Ente per le Nuove tecnologie,
l'Energia e l'Ambiente

Ministero dello Sviluppo Economico

RICERCA SISTEMA ELETTRICO

Characterization of Nano-Ashes Generated during Pulverized Coal Combustion

F. Carbone, R. Pagliara, A.C. Barone, F. Beretta, A. D'Anna

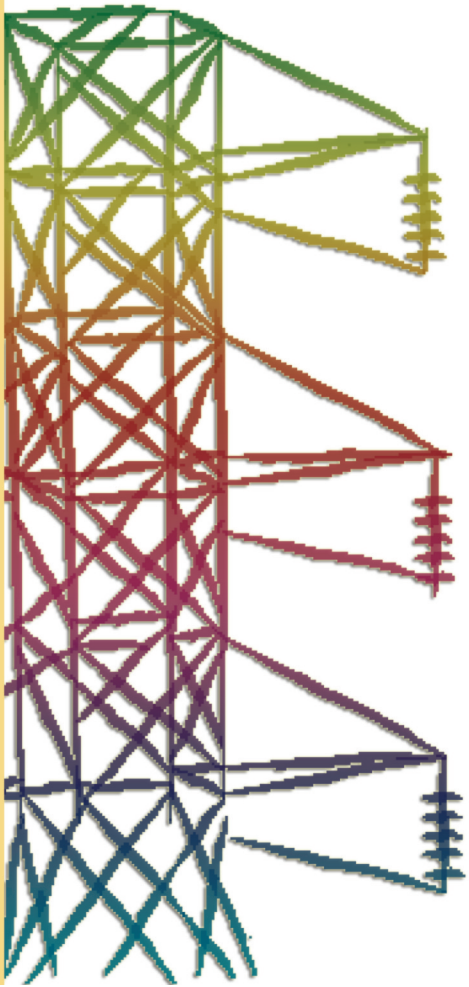

Report RSE/2009/109

Ente per le Nuove tecnologie,
l'Energia e l'Ambiente

Ministero dello Sviluppo Economico

RICERCA SISTEMA ELETTRICO

Characterization of Nano-Ashes Generated during Pulverized Coal Combustion

F. Carbone, R. Pagliara, A.C. Barone, F. Beretta, A. D'Anna

Report RSE/2009/109

CHARACTERIZATION OF NANO-ASHES GENERATED DURING PULVERIZED COAL COMBUSTION

F. Carbone, R. Pagliara, F. Beretta (Istituto di Ricerche sulla Combustione del C.N.R. – Napoli)

A.C. Barone (Istituto Italiano di Tecnologia – IIT – Genova)

A. D'Anna (Dipartimento di Ingegneria Chimica dell'Università di Napoli Federico II)

Aprile 2009

Report Ricerca Sistema Elettrico

Accordo di Programma Ministero dello Sviluppo Economico - ENEA

Area: Produzione e fonti energetiche

Tema: Tecnologie innovative per migliorare i rendimenti di conversione delle centrali a polverino di carbone - Sviluppo di un sistema di combustione di tipo "flameless" per impianti di produzione di elettricità con ridottissimi livelli di emissione di inquinanti e CO_2

Responsabile Tema: Stefano Giammartini, ENEA

Characterization of Nano-Ashes Generated During Pulverized Coal Combustion

F. Carbone[1], R. Pagliara[1], A.C. Barone[2], F. Beretta[1], A. D'Anna[3]

1. Istituto di Ricerche sulla Combustione - C.N.R., Napoli – ITALY
2. Istituto Italiano di Tecnologia (IIT), Genova - ITALY
3. Dipartimento di Ingegneria Chimica - Università Federico II, Napoli - ITALY

1. Introduction

Coal fired boilers are widely used for electric utilities and power plants because of the low cost and the abundance of this fuel. The major drawbacks of coal combustion are connected with the emissions of fine particles (size smaller than 2.5μm), nitrogen oxides and carbon dioxide. Alternative reactor configurations are being investigated to enhance energy efficiency and reduce greenhouse-gas and pollutant emissions. One of the most promising is atmospheric-pressure pulverized coal combustion in mixtures of oxygen and recirculated flue gas. This technology, attractive because of the possibility to convert conventional plants, requires enhanced oxygen levels. The ash formation in coal-air furnaces has been studied extensively [1-4] but only few researches have reported the size distribution of submicron particles generated from coal combustion in oxygen enriched conditions [5]. The ultrafine fraction (D<100nm) of coal fly ash has the highest impact on human health since toxicological results have shown that particles toxicity increases with decreasing particles size and depends on their number concentration [6]. Also the efficiency of the filtering devices decreases with decreasing particles size [7] suggesting that ultrafine ashes, once generated, are almost totally dispersed in the atmosphere. Despite these evidences nanoparticles with size smaller than 30nm have always been neglected. This fraction was not taken in consideration because of two reasons. Firstly commercial diagnostic do not detect such small particles. On the other hand it is assumed that their intense Brownian coagulation does not allow them to survive at the exhaust so that they have negligible mass concentration at the coal furnace stack. Recent advances in diagnostics showed that, at high temperature, the coagulation rate of nanoparticles drops dramatically by orders of magnitude for size below 10nm both for carbonaceous [8] and metal nanoparticles [9-11]. For this reason nanosized ashes could survive at exhaust conditions and be emitted in the atmosphere in not negligible amount. In this paper we present an experimental study on ultrafine particles formed during high-temperature pulverized coal combustion. Size distribution functions measurements in this size range were performed to this aim on a laboratory flow reactor designed on purpose.

2. Experimental

2.1. Flat premixed flame reactor

The reactor consists of a fuel lean flat laminar premixed flame homogeneously doped with pulverized coal particles, monodisperse in size. The flame is operated at atmospheric pressure. This reactor ensured that coal combustion and ash formation proceed, on average, only as a function of the height above the burner (HAB). A high volatile bituminous coal is milled in a Planetary Mono Mill (Pulverisette 6, Fritsch) and subsequently suspended in ethanol. The suspension, with coal mass concentration of about 2%, was intensively sonicated to fragment agglomerated coal particles. More than 95% of the coal particles have size smaller than 30μm

as verified by the granulometric analysis performed on the suspension (Particle Sizing System Hydro 2000S, Malvern Instrument). A Berglund-Liu-type Vibrating Orifice Aerosol Generator (VOAG model 3450, TSI) is used to generate 80μm monodisperse droplets of the coal suspension. The VOAG syringe pump is partially immersed into an ultrasonic bath, providing the suspension stability, while providing a constant suspension flow of 0.30cm^3/min through a 40μm orifice oscillating at a frequency of 20KHz. The droplets are suddenly dispersed into 2.3l/min (STP) of O_2, preventing their coalescence. The resulting aerosol is fed to the burner. The burner is similar to that used by Arabi-Katbi et al. [12] and it consists of two coaxial stainless steel tubes. The inner tube (18mm ID) is thermostated at 90°C and carries the reacting mixture. A 40mm long Mullite Zirconia honeycomb (400CPSI, CTI s.a.) is placed on the top of it. The outer tube supplies a ring (24mm ID and 34 OD) used for flowing 9l/min (STP) of the sheath Ar. A flat plate is also placed at HAB=90mm.
Ethanol completely evaporates through the honeycomb. The gaseous mixture is burned in a lean flame with equivalence ratio of about 0.15 stabilized on the honeycomb mouth. The monodisperse coal particles generated by ethanol evaporation, are carried by the gaseous stream into the flame. Coal particles devolatilize, ignite and oxidize at high temperature, downstream of the flat flame front, into the burnt gas mixture composed by 77.5% of oxygen, 13.5% of water and 9.0% of carbon dioxide (vol. %). Flow reactor temperature is measured on-axis downstream the flames front using a 250μm Pt/Pt-13%Rh thermocouple (Type R, Omega Engineering). The measured temperature profile, properly corrected for the radiative losses, is shown in Fig.1. Temperature profile is measured feeding pure ethanol to avoid particle deposition on the thermocouple junction. Particle residence times in the reactor (RT) are calculated assuming particles velocity equals to that of hot gases.

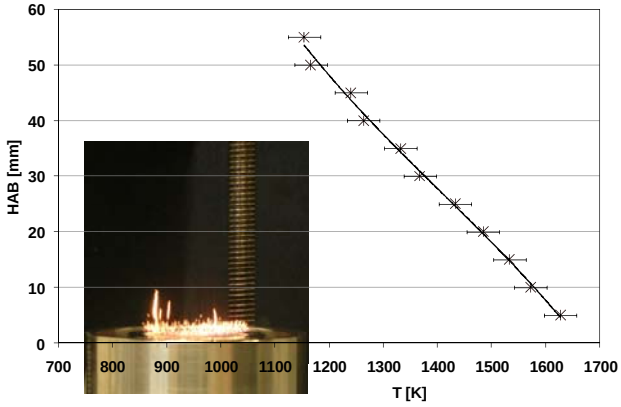

Fig. 1 Photograph of the flame reactor and its temperature versus height above the burner.

Figure 1 also shows a photograph of the flame and thus of coal particles combustion trajectories. The premixed flat flame zone is evidenced by the blue light emission just on the mouth of the burner. Char particle combustion is evidenced by the yellow colored strikes due to incandescent light emission from their surface. Coal ignition occurs very fast (RT ~1ms) because the luminous strikes are visible beginning from low HAB (1mm) in the reactor. Char burnout, evidenced by the endpoint of the incandescent traces of the particles, on average occurs at HAB~3mm and thus requires about 3ms, a time much shorter than that reported in the literature because of the smaller sizes of the fed coal particles [13]. Some larger and more persistent coal particles are visible on the edge of the reactor. This agglomerates form on burner walls and are carried into the flame by cold gasses. Measurements are not affected by these random perturbations because samplings are performed on the reactor axis at HAB=50mm. The image shows that coal devolatilization and char ignition and oxidation have almost completely run out at this HAB corresponding to a residence time of about 65ms.

2.2. Differential Mobility Analysis

The size distribution functions of ultrafine coal generated particles are on-line measured using a dilution probe and a TapCon 3/150 Differential Mobility Analyzer (DMA) system equipped with a Faraday Cup Electro-meter detector 13. The measurements were performed operating the DMA in two modality with nominal mobility diameter (MD) measurements range from 0.6nm to 28nm and from 2.1nm to 100nm, respectively.

We used horizontal tube rapid dilution probes (8mm ID, 0.5mm wall thickness) to suddenly cool and dilute sampled aerosol and transport them to the DMA [14-17]. The aerosol was drawn through a pinhole, drilled on the probe walls, while 29.5l /min of particle free dilution nitrogen steadily flows into the tube. The Dilution Ratio (DR) was regulated performing a slight underpressure in the probe, manually controlled with a rotary vane vacuum pump. Three probes, with 0.3mm, 0.8mm and 1.5mm sampling pinhole diameters, were used to obtain DRs that vary more than an order of magnitude. Sampling flow rates obtained with 0.8mm and 1.5 pinhole diameter probes were evaluated by scaling the sampling flow rate obtained with the 0.3mm pinhole probe assuming equal sampling velocities at equal underpressures. Indeed the latter probe was previously calibrated by measurements of carbon dioxide concentration into the probe itself [14]. The corresponding dilution ratios, evaluated using the value of $\sim 3 \cdot 10^4$ reported in literature for the 0.3mm pinhole probe [15], were $\sim 4 \cdot 10^3$ and $\sim 1 \cdot 10^3$ with the 0.8mm and 1.5mm pinhole probe, respectively. Particle coagulation in the probe may significantly change the shape of the size distribution function of the formed particles [16,17]. Particle coagulation is suppressed by varying the DR in order to attain a critical value, above which the shape of the size distribution does not change, that unfortunately reduces the concentration of the particles larger than 30 nm to concentrations at the detection limit of the electrometer. This effect limits somewhat the possibility of simultaneously characterizing particles in the whole ultrafine size range. Measurements in the nominal MD range from 0.6nm to 28nm were performed using the 0.3mm and 0.8mm pinhole probes while the range from 2.1nm and 100nm was investigated at lowest DRs.

The number size distribution functions of aerosol in flame are obtained multiplying the measured size distribution functions for the applied dilution ratio. Each point of this distribution is multiplied by the corresponding particles volume to obtain the volume fraction distribution. The volume is calculated considering that MD is slightly larger than the particles real diameter (D_0=0.5 nm) [18]. The particles number concentration and volume fraction are calculated by integrating the obtained size distribution functions in the desired MD intervals.

2.3. Atomic Force Microscopy Dimensional Analysis

Coal generated particles are thermophoretically collected on mica muscovite disks (3mm diameter and 0.2mm thick) inserted parallel to the gas streamline using a properly designed pneumatic actuator that assures a quick insertion and a constant sampling time ($\Delta t \sim 30$ms). The samples are analyzed by an atomic force microscope (Nanoscope IIIa™, Digital Instruments) operating in tapping-mode. A topological three-dimensional image of the deposited particles is generated with a resolution of about 1-2 nm for x/y axes and below 0.1nm for the z axis [8,9]. An advanced image processing software (S.P.I.P.™, ImageMetrology) obtains the particles volumes, baseline areas, and maximum heights above the substrate. Particle diameter and Aspect Ratio (AR) are calculated as the diameter of a sphere having the measured volume and the height to baseline diameter ratio, respectively. Results are converted in a normalized frequency size distribution function performing particles count in proper diameter intervals. The particles number concentration is also calculated by means of thermophoretic theory and is used to obtain the not normalized size distribution function [10,11].

3. Results and discussion

The size distribution functions, measured with the DMA at several DRs, are shown in fig. 2 both in number and volume concentrations. Particles larger than 30nm are not revealed using the highest DRs because their number concentration in the probe decreases below the electrometer sensitivity. The size distribution functions for mobility diameter smaller than 1nm are not reported due to artifacts contribution. The sub-nanometric matter also gives a negligible contribution to calculated volume fraction in all investigated cases [14].

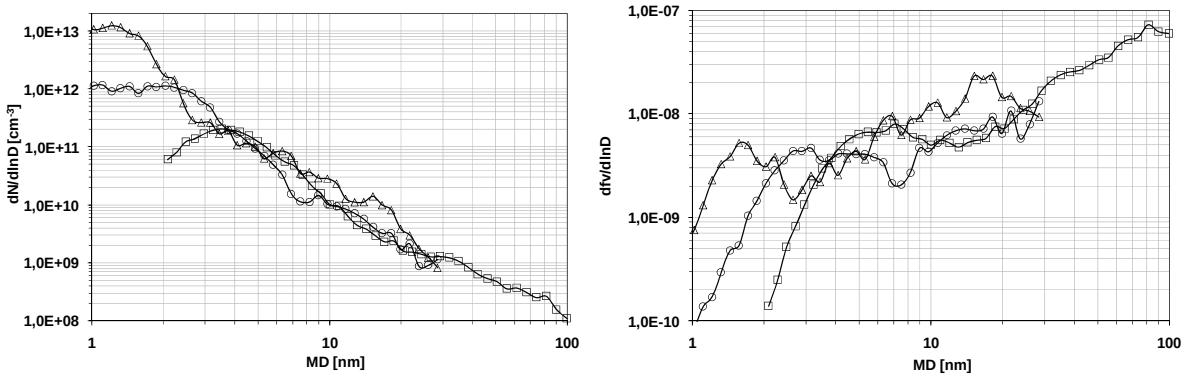

Fig. 2 Number (left) and volume (right) size distribution functions measured with the DMA. (Δ DR~3·10⁴; □ DR~4·10³; ○ DR~1·10³).

The biggest differences among the results are observable for size smaller than 3nm. The particles in this size range are the most abundant at the highest DR while they quickly disappear with decreasing DR because of their intense Brownian coagulation into the probe. The size distribution functions show almost the same profile for MD larger than 4nm. Particles number concentration quickly falls down of four orders of magnitude with increasing size up to 100nm. The measured ultrafine ash size distribution functions, in volume, evidence at least four modes roughly centered at 1.5nm, 5nm, 20nm and 80nm. The 80nm mode can be observed only using the DMA in the 2nm to 100nm size range while the 1.5nm mode progressively disappears with lowering of dilution.

The number concentration of particles with size between 1nm and 30nm, calculated integrating the measured size distribution functions, are $6\cdot10^{12}$cm^{-3} and $2\cdot10^{12}$cm^{-3} at the highest and intermediate dilutions, respectively. At the lowest dilution the number concentration of particles between 2nm and 30nm is much lower ($2\cdot10^{11}$cm^{-3}) because of coagulation. In all cases more than 98% of those nanoparticles have size smaller than 10 nm. Particles larger than 30nm, detected only at the lowest DRs, are a negligible number fraction of ultrafine ashes being $6\cdot10^{8}$cm^{-3}. The volume fraction of ultrafine particles, calculated integrating the size distribution obtained at the lowest dilution, is about $6\cdot10^{-8}$. Nanoparticles smaller than 30nm represent a fraction of ultrafine particles volume comprised between a third and a fifth while the volume fraction of nanoparticles smaller than 10nm is $7\cdot10^{-9}$ regardless of the used dilution.

The total ash mass concentration can be easily evaluated performing a material balance on the flow reactor and it is $1.7\cdot10^{-7}$g/cm^{3}. This imply that, assuming unitary density for ultrafine ashes, ultrafine particles represent about the 35% of total fed ashes mass while nanoparticles smaller than 10nm represent about the 4% of total. These high percentages are only indicative because of the strong approximation on ultrafine ashes density and because of uncertainties on the applied dilution ratios. The small size of coal fed in the flow reactor (aggregates of 20μm) respect to that commonly used in practical pulverized coal combustors could promote ultrafine ashes respect to larger particle formation. However ultrafine and nano fractions

represent a not negligible amount of total ashes even in mass concentration.
Generated particles were also collected on mica substrates to perform their AFM analysis. Each image, one shown in fig.3, contains about thirty particles. The aspect ratio of all collected particles is also plotted in fig.3 versus their diameter. The aspect ratio decreases with decreasing size and it is lower than 0.1 for diameter smaller than 10nm. This behavior was already observed for metal nanoparticles [9-10]. Particles larger than 30nm were not collected because of their low number concentration.

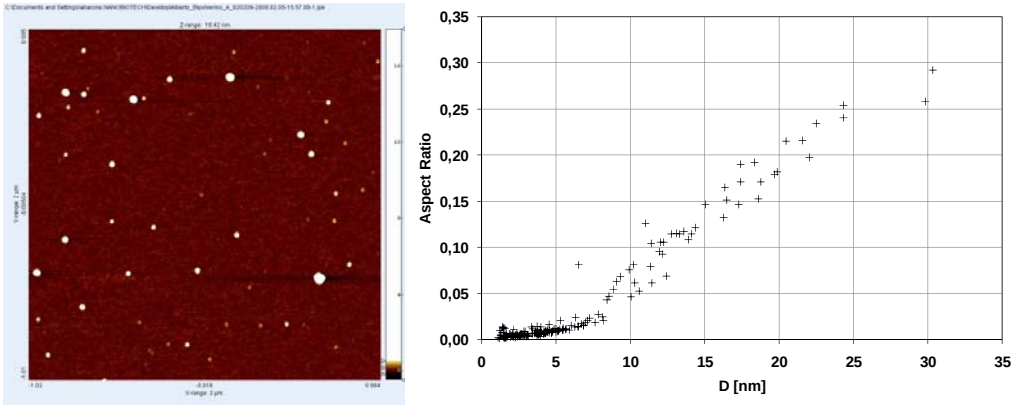

Fig. 3 AFM image (left) and Aspect Ratios (right) of particles collected on mica substrate.

The number concentration of particles smaller than 30nm obtained by AFM analysis is $1.5 \cdot 10^{10} cm^{-3}$ and it is between two and three orders of magnitude lower than that obtained with the DMA. The not normalized size distribution function of collected particles is plotted in fig.4. It agrees with those measured with DMA, reported in dotted and dashed lines, for mobility diameter larger than 10nm. AFM analysis counts a number of particles increasingly lower than that detected by the DMA for mobility diameters smaller than 10nm and about three orders of magnitude lower for MD=2nm. This increasing discrepancy could be related to the decrease of collection efficiency with decreasing diameter observed both for carbonaceous [8] and metal nanoparticles with size smaller than 10nm [9-11].

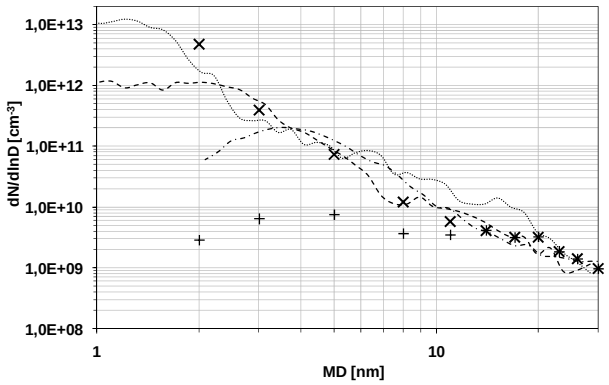

Fig. 4 Size distribution function obtained by AFM image analysis compared to those measured with the DMA. (+ not corrected; × corrected for collection efficiency).

The size distribution function obtained with AFM analysis was corrected using the profile of collection efficiency reported in literature for NiO nanoparticles [11]. The corrected size distribution function is also plotted in fig.4 and it agrees very well in the size range from 2nm to 30nm with that measured with the DMA using the highest dilution.

4. Conclusions

This study concerns the development of a new laboratory reactor allowing to investigate nano-ash from high temperature coal combustion in oxygen enriched conditions. It consists of a fuel lean flat laminar premixed flame homogenously doped with pulverized coal particles. The size distribution functions of particles down to 1nm were measured with DMA and particles sampling for AFM analysis. The results clearly showed that ultrafine particles have a very high number concentration so that they cannot be neglected. Moreover nanoparticles smaller than 10nm are the most abundant in number and they also give a not negligible contribution to total ashes volume fraction.

5. Acknowledgements

The work was partially supported by Ministry of Economical Development (MSE, Italy) under the Accordo di Programma CNR - MSE "Gruppo Tematico Carbone Pulito: Tecnologie innovative per migliorare le prestazioni ambientali delle centrali a polverino di carbone". The authors thank Claudio Canale of the IIT Genova to perform AFM imaging of samples and the undergraduate students Fabio Brando and Raffaele La Gala of the Università degli Studi di Napoli Federico II for the help in performing the measurements.

6. References

1. Sarofim A.F., Howard J.B., Padia A.S.: *Combust. Sci. Technol.* **16**:187 (1977).
2. Quann R.J., Sarofim A.F: *Proceedings of The Combustion Institute* **19**:1429 (1982).
3. Helble J. J., Sarofim A. F.: *J. Colloid Interface Sci.* **128**:348 (1989).
4. Linak W.P., Miller C.A., Seames W.S., Wendt J.O.L., Ishinomori T., Endo Y., Miyamae S.: *Proceedings of The Combustion Institute* **29**:441 (2002).
5. Biswas P., Wu C.Y.: *J. Air & Waste Manage. Assoc.* **55**:708 (2005).
6. Oberdorster G., Oberdorster E., Oberdorster J.: *J. Environ. Health Perspectives* **113**:823 (2005).
7. Suriyawong A., Gamble M., Lee M.H., Axelbaum R., Biswas P.: *Energy Fuels* **20**:2357 (2006).
8. D'Alessio A., Barone A.C., Cau R., D'Anna A., Minutolo P.: *Proceedings of The Combustion Institute* **30**:2595 (2005).
9. Carbone F., Barone A.C., Pagliara R., Beretta F., D'Anna A., D'Alessio A.: *Environ. Eng. Sci.* **25**(10):1379 (2008).
10. Carbone F., Barone A.C., Beretta F., D'Anna A., D'Alessio, A.: *32nd Symposium on Combustion of The Combustion Institute*, McGill University, Montreal, Canada (2008).
11. Carbone F., Barone A.C., De Filippo A., Beretta F., D'Anna A., D'Alessio A.: *Chem. Eng. Transactions* **16**:87 (2008).
12. Arabi-Katbi O.I., Morrison P.W., Megaridis C.M, Pratsinis S.E.: *Combust. Flame* **124**:560 (2001).
13. Murphy J.J., Shaddix C.R.: *Combust. Flame* **144**:710 (2006).
14. Sgro L.A., De Filippo A., Lanzuolo G., D'Alessio A.: *Proceedings of The Combustion Institute* **31**:631 (2007).
15. Minutolo P., D'Anna A., D'Alessio A.: *Combust. Flame* **152**:287 (2007).
16. Kasper M., Siegmann K., Sattler K.: *J. Aerosol Sci.* **28**:1569 (1997).
17. Maricq M.M.: *Combust. Flame* **137**:340 (2004).
18. Fernadez de la Mora J.J., De Juan L.L., Liedtke K., Schmidt-Ott A.: *J. Aeros. Sci.* **34**:79 (2003).